

Article

Synthesis of ZnO Nanorods at Very Low Temperatures Using Ultrasonically Pre-Treated Growth Solution

Khairul Anuar Wahid ^{1,*}, Irfan Abdul Rahim ^{2,3}, Syafiqah Nur Azrie Safri ^{4,5}  and Ahmad Hamdan Ariffin ^{4,5,*} 

¹ Mechanical Engineering Section, Universiti Kuala Lumpur Malaysia France Institute, Bandar Baru Bangi 43650, Selangor, Malaysia

² Faculty of Mechanical Engineering Technology, Universiti Malaysia Perlis, Kampus Tetap Pauh Putra, Arau 02600, Perlis, Malaysia

³ Green Design and Manufacture Research Group, Center of Excellence Geopolymer and Green Technology (CEGeoGTech), Universiti Malaysia Perlis, Kangar 01000, Perlis, Malaysia

⁴ Research Centre for Unmanned Vehicle (ReCUV), Faculty of Mechanical and Manufacturing Engineering, Universiti Tun Hussein Onn Malaysia (UTHM), Parit Raja 86400, Johor, Malaysia

⁵ Department of Aeronautical Engineering, Faculty of Mechanical and Manufacturing Engineering, Universiti Tun Hussein Onn Malaysia (UTHM), Parit Raja 86400, Johor, Malaysia

* Correspondence: khairulanuarabdwahid@unikl.edu.my (K.A.W.); ahmadh@uthm.edu.my (A.H.A.)

Abstract: This paper investigates how the pre-treatment of the growth solution with ultrasonic energy affects the annealing temperatures and the growth temperatures of zinc oxide (ZnO) nanorods. The ultrasonic pre-treatment of the growth solution resulted in the successful growth of ZnO nanorods at a very low annealing temperature of 40 °C. The size and density of ZnO nanorods were found to increase proportionally with the increasing duration of pre-ultrasonic treatment, as indicated by characterisations performed with a scanning electron microscope (SEM). At an annealing temperature of 40 °C, coupled with ultrasonic waves, the SEM results showed that ZnO nanorods' length and diameter increased by 37 and 25%. A similar pattern was also observed at an annealing temperature of 60 and 80 °C, where the length and diameter of ZnO nanorods increased. In addition, the conductivity and acidity of the aqueous solution that had been sonicated were measured. The results showed that solution conductivity and acidity increased as the ultrasonic treatment continued for longer periods. After 3 min of sonication, the final conductivity and acidity of the solutions were found to be 9164 $\mu\text{S}/\text{cm}$ and 6.64, respectively. The results also indicated that the ultrasonic pre-treatment of the growth solution increased the zinc nutrient concentration, which would affect the formation of ZnO nanorods. In addition to the ultrasonic effect, the annealing temperature influenced the active nucleation sites essential to the ZnO nanorods' expansion.

Keywords: ultrasonication method; zinc oxide (ZnO); nanorods; low-temperature process; photocatalytic degradation



Citation: Wahid, K.A.; Rahim, I.A.; Safri, S.N.A.; Ariffin, A.H. Synthesis of ZnO Nanorods at Very Low Temperatures Using Ultrasonically Pre-Treated Growth Solution. *Processes* **2023**, *11*, 708. <https://doi.org/10.3390/pr11030708>

Academic Editors: Maria José Lo Faro, Alessia Irrera and Rosaria Anna Picca

Received: 31 January 2023

Revised: 23 February 2023

Accepted: 24 February 2023

Published: 27 February 2023



Copyright: © 2023 by the authors. Licensee MDPI, Basel, Switzerland. This article is an open access article distributed under the terms and conditions of the Creative Commons Attribution (CC BY) license (<https://creativecommons.org/licenses/by/4.0/>).

1. Introduction

Zinc oxide (ZnO) nanostructures have gained much attention from researchers and industrialists because of their remarkable properties, including high binding energy, wide band gap, high thermal resistivity, photoluminescence, and piezoelectric effect [1]. These properties have highlighted ZnO as a potential material for various applications, such as in solar cells [2], photocatalysts [3], electrochemical sensors [4], gas sensors [5], and energy harvesters [6]. The size, shape, and quantum confinement effect of the ZnO nanostructure provide a variety of remarkable and intriguing characteristics. It is also among the most promising materials for a range of microelectronic and optoelectronic devices due to its broad band-gap energy, high excitation binding energy, and lack of central symmetry [7]. ZnO nanostructures can be prepared using various synthesis techniques, such as chemical vapor deposition (CVD) [8], electrochemical deposition [9], sputtering

deposition [10], and pulse laser deposition [11]. These synthesis techniques can produce high-quality ZnO nanostructures but require severe reaction conditions, including high temperature (beyond 400 °C), precise gas concentration, rigid gas flow rate, and strict process control [12]. For sensor applications, a platform made from a flexible material is necessary to allow the integration of the ZnO nanostructures with portable consumer devices, thereby facilitating the key features of enhanced appearance, trendiness, and light weight. Thus, a low-temperature synthesis process is required to produce the nanomaterial because flexible substrates are typically unable to withstand high process temperatures and extreme processing conditions.

Hydrothermal synthesis is a low-temperature technique in which ZnO nanostructure growth can be achieved at temperatures below 100 °C. The hydrothermal synthesis setup is simple and experimentally proven for large-area nanostructure growth [13]. Although the growth temperature is low in such a system, the ZnO-seed layer annealing temperature before final growth is still high, typically between 100 and 450 °C (e.g., Sheng et al. at 300 °C for 20 min [14], Sunandan et al. at 450 °C for 5 h [15], Hu et al. at 180 °C for 1 h and 300 °C for 30 min [16], and Min et al. at 300 °C for 10 min before and after depositing the ZnO seed layer [17]). An alternative hydrothermal synthesis technique for ZnO-nanorod growth can avoid the need for a seed layer during annealing. This alternative process is a single-step solution wherein an autoclave introduces high pressure and energy density to a small confined area during growth [18]. However, this autoclave process only allows growth over large areas, particularly at wafer-scale levels. Moreover, the single-step solution process usually requires very long growth times (e.g., Balasubramaniam et al. required 10 h at 90 °C [19], Liu et al. required 24 h at 95 °C [20], Li et al. required 12 h at 180 °C [21], and Conghua et al. required 18 h at 150 °C [22]).

The sonochemical method utilises the high intensity of ultrasound. It offers a facile versatile synthetic tool for nanostructured materials at room temperature with a growth duration of one to three hours [23–25]. During the growth process, the ultrasonic treatment is applied to the growth solution. However, the deposited metal or resist may be damaged due to long-duration exposure to ultrasound and this may affect the patterning growth process [26]. To address these issues, a new approach was developed. The growth solution is treated first with ultrasound at room temperature before the growth process is carried out via the hydrothermal method. Applying ultrasound to the growth solution improves the dilution of zinc nutrients in the aqueous mixture. As shown in the later sections of this paper, the application of ultrasound assists the ZnO nanostructure growth at very low process temperatures. This method provides an alternative method to grow ZnO nanostructures at a very low annealing temperature and with minimum equipment. This is important, as the low-temperature process is necessary because the flexible substrates mostly have a low melting point.

2. Materials and Methods

ZnO nanostructures were synthesised by hydrothermal growth on oxidised silicon (SiO₂) substrates. The catalyst, which acts as a seed layer to form the ZnO nanorods, was prepared using a mixed solution of 0.2 M zinc acetate dehydrate and diethanolamine in ethanol. The materials used were zinc acetate dihydrate powder with a molecular weight of 299.51, diethanolamine powder with a molecular weight of 105.14, zinc nitrate hexahydrate with a molecular weight of 297.49, and hexamethylenetetramine powder with a molecular weight of 140.19. The solution was then spin-coated onto the SiO₂ surface at a speed of 3000 rpm for 30 s. To investigate the minimum annealing temperature (AT) required to grow the ZnO nanorods, SiO₂ samples coated with a Zn seed layer were annealed at 40, 60, and 80 °C for 1 h using ceramic furnace model Muffle LE 14/. For the growth nutrient solution, 0.04 M aqueous solutions comprising zinc nitrate hexahydrate and hexamethylenetetramine mixed in de-ionised (DI) water were prepared and sonicated for 5 s and 3 min. The reason for these sonication times was to investigate the potential of sonication to facilitate the ZnO growth over a short period.

Ultrasonic model Branson CPX1800-J was used to sonicate the prepared solution at a fixed frequency of 1000 Hz for 5 s and 3 min, respectively. Considering the ultrasonication equipment's limitations, the ultrasonic bath's power frequency was fixed at 40 kHz. The position of the beaker containing the aqueous solution was selected, and all of the beakers used for this experiment were of the same size and volume to ensure that the intensity of the sonication power was applied equally to each sample. After sonication, the annealed samples were immersed in the aqueous solution vertically. Final ZnO nanorod growth was conducted at temperatures of 40, 60, and 80 °C for 3 h. Ph meter model Benchtop S400 was used to measure the effect of pH value after the solution had been sonicated for different periods. The following sections discuss ZnO nanostructure growth results in sonicated and unsonicated solutions. Ultra-high resolution field emission–scanning electron microscopy (FE-SEM) SU9000 was used to observe ZnO nanorod growth, and atomic force microscopy with RAMAN (AFM) was used to characterise the surface roughness of the seed layer after the annealing process.

3. Results and Discussions

The ultrasonication process yields acoustic cavitation, which helps speed up the chemical reaction in the Zn aqueous solution. Acoustic cavitation occurs when an ultrasonic wave is transmitted through liquid via vibrational pressure waves, which periodically compress and stretch the liquid's molecular structure. Hence, if a solid substance is present in this liquid solution, solid disruption diminishes the particle during the cavitation process, which increases the total solid surface area in contact with the solution [27]. The dissociation process occurs rapidly and effectively, increasing the total dissolved substance in the solution. An ultrasonic wave was applied to dissolve the ZnO powder (zinc acetate dehydrate and hexamethyltetraamine) in ethanol. In this case, more ZnO nutrients would be present in the final solution, consequently improving the ZnO nanorod growth process. Figures 1–3 show the SEM images of ZnO nanorods grown under different ultrasonic-wave durations subjected to different annealing and growth temperatures.

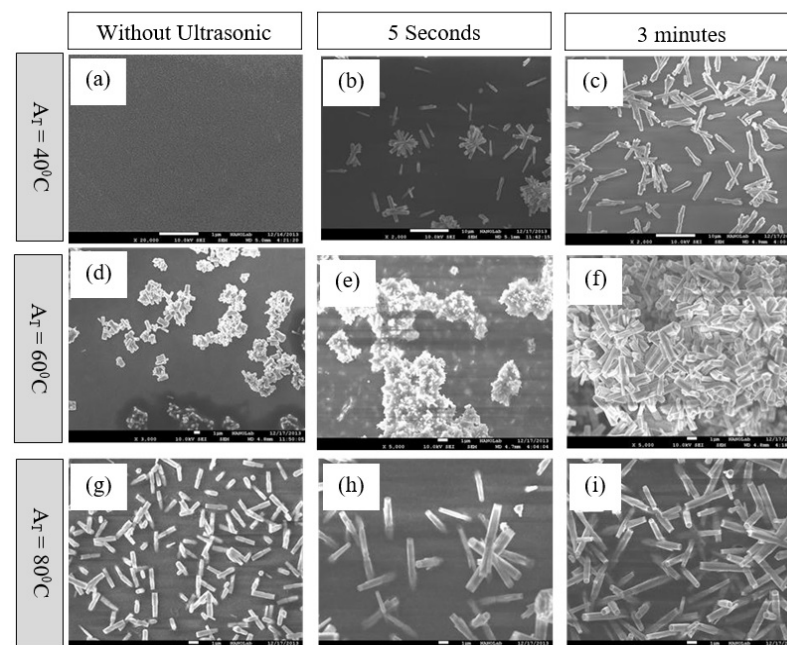


Figure 1. ZnO nanorods were grown at 80 °C and subjected to different annealing temperatures: (a–c) 40 °C, (d–f) 60 °C, and (g–i) 80 °C.

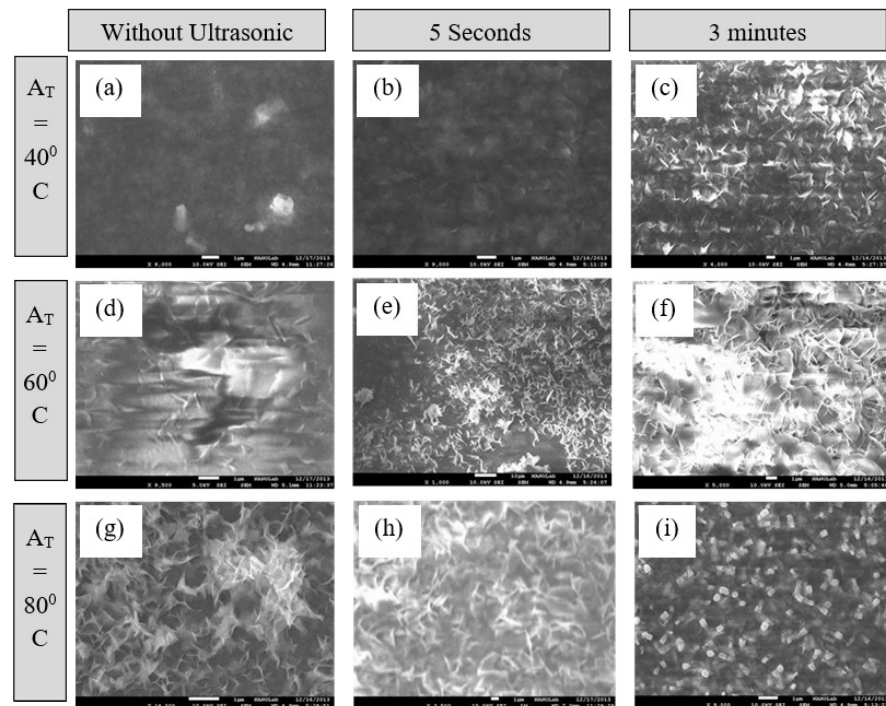


Figure 2. ZnO nanorods were grown at $60^\circ C$ and subjected to different annealing temperatures: (a–c) $40^\circ C$, (d–f) $60^\circ C$, and (g–i) $80^\circ C$.

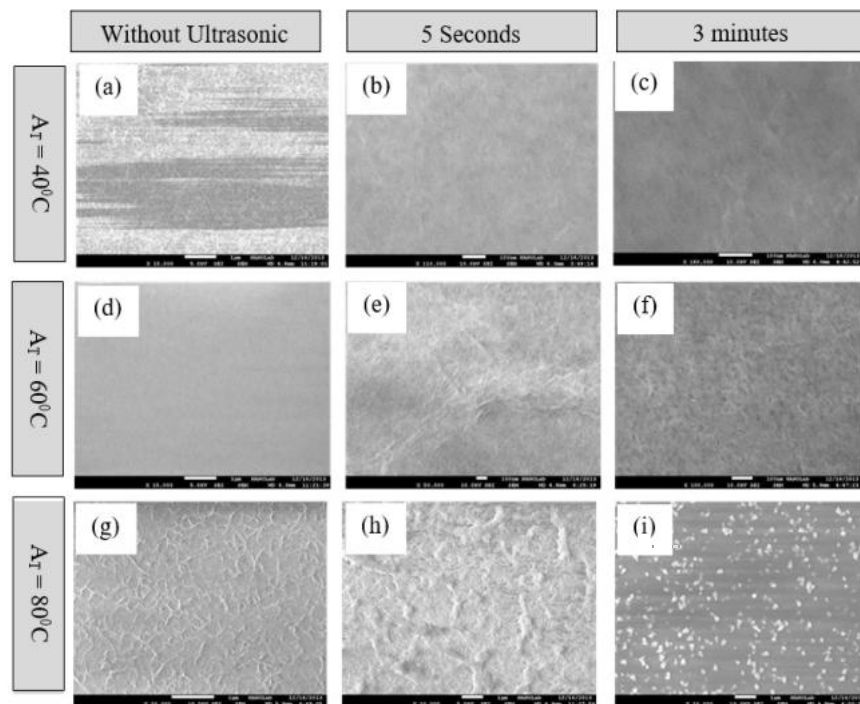
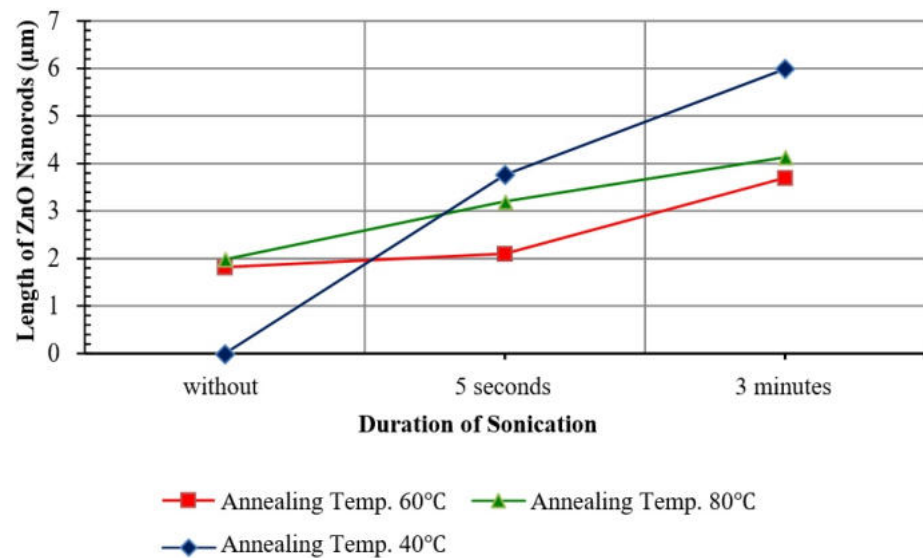
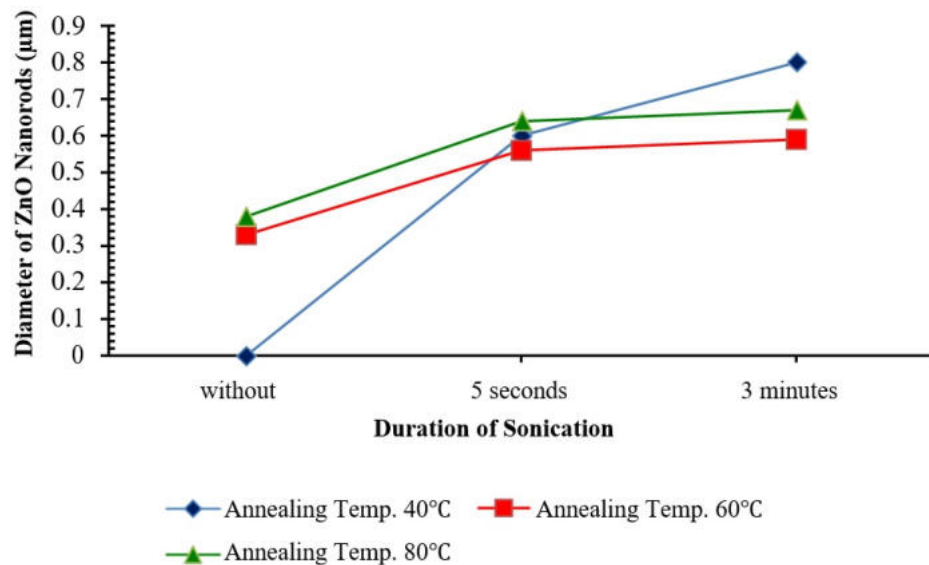


Figure 3. ZnO nanorods were grown at $40^\circ C$ and subjected to different annealing temperatures: (a–c) $40^\circ C$, (d–f) $60^\circ C$, and (g–i) $80^\circ C$.

Ultrasonic waves allow the growth of ZnO nanostructures at very low annealing temperatures (40 °C). However, ZnO nanorods were only observed when the growth temperature was 80 °C, as shown in Figure 1g–i. No nanorod structures were observed at 60 and 80 °C growth temperatures (Figures 2 and 3). The density and size of the ZnO nanorods that were grown increased with ultrasonic wave duration (Figure 1). Figure 4a,b summarise the average length and diameter of ZnO nanorods grown in a solution that was sonicated for 5 s and 3 min.



(a)



(b)

Figure 4. (a) The average length of ZnO nanorods grown in a solution sonicated for different lengths of time. (b) The average diameter of ZnO nanorods grown in a solution sonicated for different lengths of time.

No ZnO nanostructures were observed in the samples annealed at 40 °C when the seed layers were grown in a solution without sonication (Figure 4a,b). However, nanorod-type structures were observed when seed layers were grown in solutions that had been sonicated for 5 s and 3 min. The length and diameter of these nanorod structures significantly increased from 3760 and 600 nm to 5990 and 800 nm after sonication, which indicates that

ultrasonic wave-assisted ZnO growth occurs at very low annealing temperatures. The results also showed that the final length and diameter of the ZnO nanorods grown in the solution sonicated for 3 min increased by over 37 and 25%, respectively, compared with those of nanorods grown in the solution that had been sonicated for only 5 s.

The same trend was observed for samples annealed at 60 °C, where the final length and diameter of ZnO nanorods increased by 50 and 44%, respectively, compared with those of nanorods grown in an unsonicated solution. For samples annealed at 80 °C, the final length and diameter of ZnO nanorods increased by over 52 and 43%, respectively, compared with those of nanorods grown in an unsonicated solution. It can be concluded that the growth rate of ZnO nanorods increases proportionally with annealing temperature based on the significant size increases observed. At annealing temperatures of 40, 60, and 80 °C, the growth rates of the ZnO nanorods increased by 37, 50, and 52%, respectively.

The length of the ZnO nanorods in samples annealed at 40 °C was greater than that of samples annealed at 60 °C and 80 °C, even though the density of the ZnO nanorods grown was lower at low annealing temperatures than at high ones. This result can be explained by the number of nucleation sites proportionally increasing with annealing temperature [28]. Hence, the sample annealed at 40 °C has fewer nucleation sites than at 60 and 80 °C. Therefore, with the same amount of Zn^{2+} and OH^- concentration, each nucleation site from the sample annealed at 40 °C will receive more Zn^{2+} and OH^- compared to the sample annealed at 60 and 80 °C. As a result, ZnO nanorod growth on the sample annealed at 40 °C is longer than on the samples annealed at 60 and 80 °C. A similar observation was also reported by [29], where ZnO nanorods length increased from 250 to 742 nm when the annealing temperature increased from 250 to 400 °C. However, a further increase in the annealing temperature of the seed layer to 450 °C resulted in the decrease in the ZnO nanorod's length to 605 nm at 450 °C.

To verify this hypothesis, the nucleation sites of the samples annealed at 40, 60, and 80 °C needed to be measured. According to Kim et al. [30], the number of nucleation sites can be pointed out based on the surface roughness of seed layers after the annealing process. The surface roughness of the seed layers annealed at 40, 60, and 80 °C was characterised by atomic force microscopy (AFM).

Figure 5 shows AFM images illustrating the roughness of the seed layers, and the roughness values are summarised in Table 1. The average roughness values of samples annealed at 40, 60, and 80 °C were 48.45, 67.81, and 221.65 nm, respectively. The seed layer surface roughness increased proportionally with annealing temperature, which confirms that more active nucleation sites are present at higher annealing temperatures, indicating that the sample annealed at 40 °C had the lowest nucleation sites of seed layers. Similar results were reported where the RMS value of seed layer roughness increased from 1.9 to 2.6 nm, when increasing temperature from 150 to 350 °C [31].

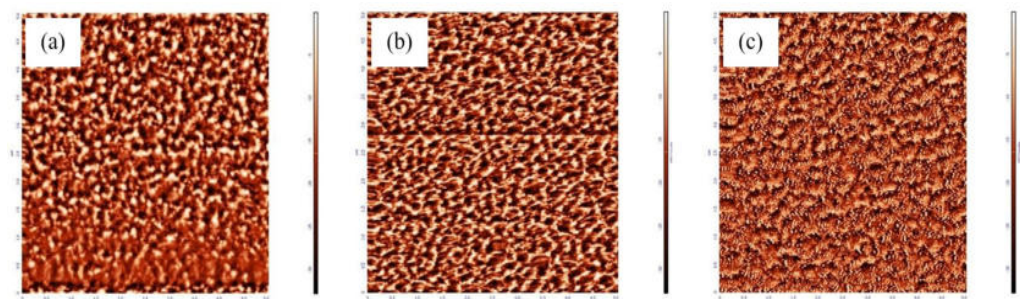


Figure 5. AFM images illustrating the roughness of the seed layers at (a) 40 °C, (b) 60 °C and (c) 80 °C.

Table 1. Surface roughness values of seed layers annealed at 40, 60, and 80 °C.

| | Annealed at 40 °C | Annealed at 60 °C | Annealed at 80 °C |
|--------------------|-------------------|-------------------|-------------------|
| Amount of sampling | 65,536 | 65,536 | 65,536 |
| Peak to peak | 293.005 nm | 410.465 nm | 1559.85 nm |
| Average roughness | 48.4501 nm | 67.8159 nm | 221.648 nm |
| Root mean square | 59.2803 nm | 83.4649 nm | 263.181 nm |

At growth temperatures of 60 and 40 °C, nanoflakes or particle-like structures instead of nanorods were formed (Figures 2 and 3). These small particles appeared similar to the initial form of nanorods, which were observed when samples were annealed at 80 °C and grown in a solution that had been sonicated for 3 min (Figures 2i and 3i). Regardless of the annealing temperature, ultrasonic waves are important in promoting ZnO nanostructure growth even at very low growth temperatures. Eventually, if the growth process is prolonged for over 3 h, these small particles will form ZnO nanorods. However, prolonging the growth duration is not an option as it will add more cost to the manufacturing process.

To understand why ultrasonic waves improve ZnO growth at very low annealing temperatures, the growth mechanism of ZnO nanostructures under ultrasonication was discussed [32]. Zinc nitrate, initially in powder form, is an ionic compound. Zinc has a positive charge (Zn^{2+}), whereas nitrate has a negative charge (NO_3^-). The zinc nitrate powder must be dissolved in DI water to convert the zinc nitrate powder into zinc nutrients in solution and allow the catalyst to attract zinc nutrients to form the desired nanostructures. DI water molecules have two component ions, which are $H_2O = H^+ + OH^-$. In general, the positive charge of H^+ and the negative charge of OH^- enable water to possess different polarities, allowing the molecules to dissolve any ionically bonded substances. Thus, the different polarities of water molecules dissolve the zinc nitrate. The positive charge of the molecules attracts the negative charge of nitrate, and the negative charge of the water molecules attracts the positive charge of zinc. The attraction of these negative and positive charges is part of the dissociation process. During the dissociation process, the bond between zinc and nitrate is broken down, thereby allowing the dissolution of the molecules in water.

Hence, using ultrasonic waves will effectively promote the dissociation process and increase the number of ions released into the solution, thereby increasing the availability of nutrients. To verify this hypothesis, an electroconductivity sensor was used to measure the conductivity of the growth solution. Electroconductivity is one of the most common methods to measure total dissolved salt powders in a solution. When zinc powder is dissolved, more ions are freed in the solution. In addition to being electroconductivity sensors, pH meters can also indicate the zinc nutrient concentration in a solution because the solution acidity increases proportionally with zinc nitrate dissolution [33]. The pH of each sonicated solution was collected at room temperature (during sonication, the solution temperature increased because of the cavitation process). Figure 6 summarises the conductivity and pH of the solutions prepared under different sonication times.

The conductivity and acidity of the solutions increased proportionally with the sonication duration (Figure 6). The initial conductivity and pH of the solutions were 16 $\mu S/cm$ and 8.68, respectively, which indicated that the solution had low ionic activity because of the limited amount of zinc powder dissolved in the solution. When the zinc powder was manually stirred for 5 min, the solutions' conductivity and acidity (pH) significantly increased to 7883 $\mu S/cm$ and 6.8, respectively. The conductivity and acidity of the solutions further increased to 8571 $\mu S/cm$ and 6.70 when the dissolution of zinc powder in the solution was extended by ultrasonication for 5s. After 3 min of sonication, the final conductivity and acidity of the solutions were found to be 9164 $\mu S/cm$ and 6.64, respectively. The conductivity of the solutions decreased to 8163 $\mu S/cm$ after the growth process because of the precipitation of zinc powder at the bottom of the beaker, which forms zinc salt crystals that decrease ion activity. The proportional increase in conductivity with sonication duration indicates that using ultrasonic waves improves the total amount of dissolved ZnO

powder in the solutions. The solution acidity increases because of the increase in H⁺ ions released during sonication [31]. As a result of the experiments that were carried out, it was discovered that using ultrasonic waves could promote higher zinc nutrient concentrations in the growth solution. This, in turn, makes it possible for the catalyst to attract more nutrients while the process is in progress. Thus, ZnO nanorods can grow even at very low temperatures.

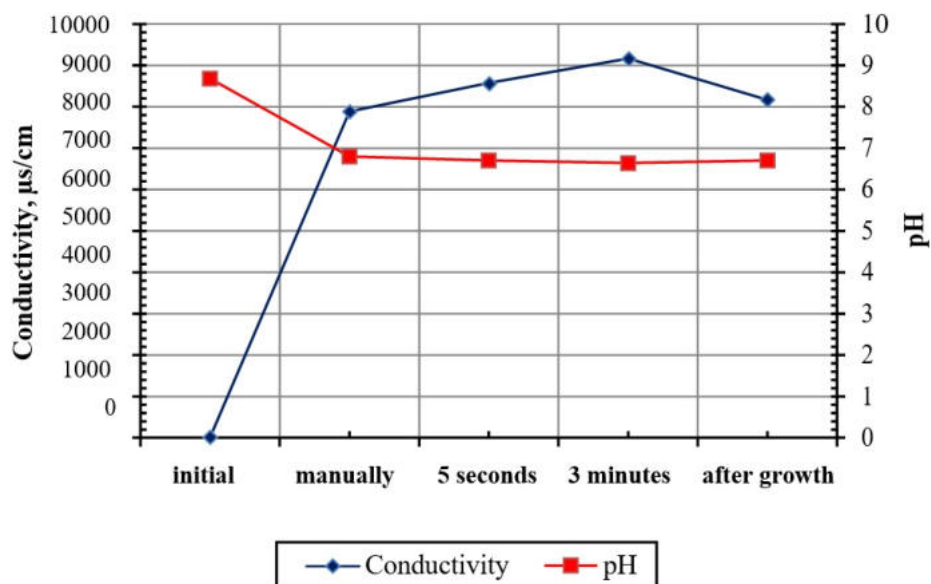


Figure 6. Conductivity and pH of the ZnO growth solutions under different sonication times.

4. Conclusions

This study presents the application of ultrasonic waves when formulating a zinc nutrient solution to improve zinc nitrate dissolution in DI water. The effect of pre-treatment growth solution with ultrasonic waves on the ZnO nanostructure growth process was investigated. The zinc nutrient concentration in the solution significantly increased using ultrasonic waves, allowing ZnO nanorods to grow at annealing temperatures as low as 40 °C. SEM images revealed that the ZnO nanorods' final length and diameter increased by 37 and 25% when subjected to an annealing temperature of 40 °C coupled with ultrasonic waves. Furthermore, the length and diameter of ZnO nanorods increased by 50 and 55%, respectively, at an annealing temperature of 60 °C and by 52 and 43% at an annealing temperature of 80 °C. Thus, besides ultrasonication, the annealing temperature also plays a crucial role in determining ZnO-nanorod size. The surface roughness analysis indicated that nucleation sites increase proportionally with increasing surface roughness, affecting the density of the ZnO nanorods that were grown.

Author Contributions: Conceptualisation, K.A.W. and I.A.R.; methodology, K.A.W. and I.A.R.; resources, K.A.W., I.A.R. and A.H.A.; writing—original draft preparation, K.A.W., I.A.R. and A.H.A.; writing—review and editing, S.N.A.S. All authors have read and agreed to the published version of the manuscript.

Funding: This work was supported by the National Nanotechnology Directorate under the Ministry of Science, Technology and Innovation Center of Excellence Program and Universiti Sains Malaysia RU (Grant No. 1001/PMEKANIK/814158) under the Ministry of Higher Education, Malaysia and part of the collaboration with MIMOS BHD and funded by STRG grant (str19024) from Universiti Kuala Lumpur.

Data Availability Statement: The data presented in this study are available on request from the corresponding author.

Acknowledgments: Communication of this research is made possible through monetary assistance by Universiti Tun Hussein Onn Malaysia and the UTHM Publisher's Office via Publication Fund E15216.

Conflicts of Interest: The authors declare no conflict of interest.

References

1. Wang, Z.L. Zinc nanostructures: Growth, properties and applications oxide. *J. Phys.* **2004**, *16*, R829–R858. [[CrossRef](#)]
2. Bykkam, S.; Kalagadda, V.R.; Kalagadda, B.; Selvam, K.P.; Hayashi, Y. Ultrasonic-assisted synthesis of ZnO nanoparticles decked with few layered graphene nanocomposite as photoanode in dye-sensitised solar cell. *J. Mater. Sci. Mater. Electron.* **2017**, *28*, 6217–6225. [[CrossRef](#)]
3. Chu, F.H.; Huang, C.W.; Hsin, C.L.; Wang, C.W.; Yu, S.Y.; Yeh, P.H.; Wu, W.W. Well aligned ZnO nanowires with excellent field emission and photocatalytic properties. *Nanoscale* **2012**, *4*, 1471–1475. [[CrossRef](#)] [[PubMed](#)]
4. Shen, G.; Chen, P.C.; Ryu, K.; Zhou, C. Devices and chemical sensing applications of metal oxide nanowires. *J. Mater. Chem.* **2009**, *19*, 828–839. [[CrossRef](#)]
5. Chang, S.J.; Weng, W.Y.; Hsu, C.L.; Hsueh, T.J. High sensitivity of a ZnO nanowire-based ammonia gas sensor with Pt nano particles. *Nano Commun. Netw.* **2010**, *1*, 283–288. [[CrossRef](#)]
6. Lu, M.P.; Song, J.; Lu, M.Y.; Chen, M.T.; Gao, Y.; Chen, L.J.; Wang, Z.L. Piezoelectric nanogenerator using p-type ZnO nanowires arrays. *Nano Lett.* **2009**, *9*, 1223–1227. [[CrossRef](#)]
7. Mohamed, M.; Sedky, A.; Kassem, M.A. Gradual growth of ZnO nanoparticles from globules-like to nanorods-like shapes: Effect of annealing temperature. *Optik* **2022**, *265*, 169559. [[CrossRef](#)]
8. Kaushik, V.K.; Mukherjee, C.; Sen, P.K. ZnO based transparent thin film transistor grown by aerosol assisted CVD. *J. Mater. Sci. Mater. Electron.* **2018**, *29*, 15156–15162. [[CrossRef](#)]
9. Elias, J.; Tena-Zaera, R.; Lévy-Clément, C. Electrochemical deposition of ZNO nanowire arrays with tailored dimension. *J. Electroanal. Chem.* **2008**, *621*, 171–177. [[CrossRef](#)]
10. Chiou, W.T.; Wu, W.Y.; Ting, J.M. Growth of single crystal ZnO nanowires using sputter deposition. *Diam. Relat. Mater.* **2003**, *12*, 1841–1844. [[CrossRef](#)]
11. Son, H.J.; Jeon, K.A.; Kim, C.E.; Kim, J.H.; Yoo, K.H.; Lee, S.Y. Synthesis of ZnO nanowires by pulsed laser deposition in furnace. *Appl. Surf. Sci.* **2007**, *253*, 7848–7850. [[CrossRef](#)]
12. Choi, H.S.; Vaseem, M.; Kim, S.G.; Im, Y.H.; Hahn, Y.B. Growth of high aspect ratio ZnO nanorods by solution process: Effect of polyethyleneimine. *J. Solid State Chem.* **2012**, *189*, 25–31. [[CrossRef](#)]
13. Wahid, K.A.; Lee, W.Y.; Lee, H.W.; Teh, A.S.; Bien, D.C.; Abd Azid, I. Effect of seed annealing temperature and growth duration on hydrothermal nanorod structures and their electrical characteristics. *Appl. Surf. Sci.* **2013**, *283*, 629–635. [[CrossRef](#)]
14. Xu, S.; Wei, Y.; Kirkham, M.; Liu, J.; Mai, W.; Davidovic, D.; Snyder, R.L.; Wang, Z.L. Patterned growth of vertically ZnO nanowire arrays on inorganic substrates at low temperature without catalyst. *J. Am. Chem. Soc.* **2008**, *130*, 14958–14959. [[CrossRef](#)] [[PubMed](#)]
15. Baruah, S.; Dutta, J. Effect of seeded substrates in hydrothermally grown ZnO nanorods. *J. Sol-Gel. Sci. Technol.* **2009**, *50*, 456–464. [[CrossRef](#)]
16. Wang, H.; Xie, J.; Yan, K.; Duan, M. Growth mechanism of different morphologies of ZnO crystals prepared by hydrothermal method. *J. Mater. Sci. Technol.* **2011**, *27*, 153–158. [[CrossRef](#)]
17. Guo, M.; Diao, P.; Cai, S. Hydrothermal growth of well-aligned ZnO nanorod arrays: Dependence of morphology and alignment ordering upon preparing conditions. *J. Solid State Chem.* **2005**, *178*, 1864–1873. [[CrossRef](#)]
18. Ho, G.W.; Wong, A.S.W. One step solution synthesis towards ultra-thin and uniform single-crystalline ZnO nanowires. *Appl. Phys.* **2007**, *86*, 457–462. [[CrossRef](#)]
19. Saravanakumar, B.; Mohan, R.; Kim, S.J. Facile synthesis of grapheme/ZnO nanocomposites by low temperature hydrothermal method. *Mater. Res. Bull.* **2013**, *48*, 878–883. [[CrossRef](#)]
20. Liu, J.P.; Xu, C.X.; Zhu, G.P.; Li, X.; Cui, Y.P.; Yang, Y.; Sun, X.W. Hydrothermally grown ZnO nanorods on self-source substrate and their field emission. *J. Phys. D Appl. Phys.* **2007**, *40*, 1906–1909. [[CrossRef](#)]
21. Li, Y.; Feng, H.; Zhang, N.; Liu, C. Hydrothermally synthesis and characterisation of tube-structured ZnO needles. *Mater. Sci.-Pol.* **2009**, *27*, 551–557.
22. Lu, C.; Qi, L.; Yang, J.; Tang, L.; Zhang, D.; Ma, J. Hydrothermal growth of large scale micropatterned arrays of ultralong ZnO nanowires and nanobelts on zinc substrate. *Chem. Commun.* **2006**, *33*, 3551–3553. [[CrossRef](#)] [[PubMed](#)]
23. Jung, S.H.; Shin, N.; Kim, N.H.; Lee, K.H.; Jeong, S.H. A sonochemical approach to the fabrication of laterally aligned ZnO nanorods field emitter arrays on a planar substrate. *IEEE Trans. Nanotechnol.* **2011**, *10*, 319–324. [[CrossRef](#)]
24. Askarinejad, A.; Alavi, M.A.; Morsali, A. Sonochemically assisted synthesis of ZnO nanoparticles: A novel direct method. *Iran J. Chem. Chem. Eng.* **2011**, *30*, 75–81.
25. Geng, J.; Song, G.H.; Zhu, J.J. Sonochemical synthesis of Er³⁺-doped ZnO nanospheres with enhanced upconversion photoluminescence. *J. Nanomater.* **2012**, *64*, 3.
26. Suslick, K.S.; Price, G.J. Applications of ultrasound to material chemistry. *Annu. Rev. Mater.* **1999**, *29*, 295–326. [[CrossRef](#)]

27. Wu, J.; Zhou, S.; Li, X. Acoustic emission monitoring for ultrasonic cavitation based dispersion process. *J. Manuf. Sci. Eng.* **2013**, *135*. [[CrossRef](#)]
28. Ondo-Ndong, R.; Ferblantier, G.; Al Kalfioui, M.; Boyer, A.; Foucaran, A. Properties of RF magnetron sputtered zinc oxide thin films. *J. Cryst. Growth* **2003**, *255*, 130–135. [[CrossRef](#)]
29. Ridhuan, N.S.; Abdul Razak, K.; Lockman, Z.; Abdul Aziz, A. Structural and morphology of ZnO nanorods synthesised using ZnO seeded growth hydrothermal method and its properties as UV sensing. *PLoS ONE* **2012**, *7*, e50405. [[CrossRef](#)]
30. Kim, J.Y.; Chang, H.; Kim, M.S.; Leem, J.Y.; Ballato, J.; Kim, S.O. Low temperature growth of multiple stack high density ZnO nanoflowers/nanorods on plastic substrates. *Nanotechnology* **2012**, *23*, 485606. [[CrossRef](#)]
31. Kim, K.H.; Utashiro, K.; Abe, Y.; Kawamura, M. Growth of Zinc Oxide Nanorods using various seed layer annealing temperature and substrate materials. *Int. J. Electrochem. Sci.* **2014**, *9*, 2080–2089.
32. Oxtoby David, W.; Pat Gillis, H.; Laurie, B. *Principles of Model Chemistry*, 6th ed.; Thomson: Stamford, CT, USA, 2008.
33. Wahab, R.; Kim, Y.S.; Shin, H.S. Synthesis, characterisation and effect of pH variation on Zinc Oxide nanostructures. *Mater. Trans.* **2009**, *50*, 2092–2097. [[CrossRef](#)]

Disclaimer/Publisher’s Note: The statements, opinions and data contained in all publications are solely those of the individual author(s) and contributor(s) and not of MDPI and/or the editor(s). MDPI and/or the editor(s) disclaim responsibility for any injury to people or property resulting from any ideas, methods, instructions or products referred to in the content.